

## Age constraints on marine-fluvial deposits at Rancho La Palma, Baja California Sur, Mexico

### Determinación de la edad de los depósitos marino-fluviales de Rancho La Palma, Baja California Sur, México

Heriberto **Rochín-Bañaga**<sup>1,\*</sup>, Donald W. **Davis**<sup>1</sup>, Tobias **Schwennicke**<sup>2</sup>,  
Atzcalli E. **Hernández-Cisneros**<sup>3</sup>

<sup>1</sup> Department of Earth Sciences, University of Toronto, 22 Russell Street, Toronto, ON M5S 3B1, 5 Canada.

<sup>2</sup> Departamento de Ciencias de la Tierra, Universidad Autónoma de Baja California Sur, 7 Km. 5.5, La Paz, Baja California Sur 23080, México.

<sup>3</sup> Instituto Politécnico Nacional, Centro Interdisciplinario de Ciencias Marinas, Av. Instituto Politécnico Nacional Playa Palo de Santa Rita, La Paz, Baja California Sur 23096, México.

\* Corresponding author: (H. Rochín-Bañaga)  
heriberto.rochinbanaga@mail.utoronto.ca

## ABSTRACT

Coastal marine and fluvial deposits, exposed at Cerro El Divisadero near Rancho La Palma, Baja California Sur, Mexico, contain a fossil record of cetaceans (baleen whales). U–Pb zircon dating of a tuff horizon collected near the base of Cerro El Divisadero yields a  $^{206}\text{Pb}/^{238}\text{U}$  age of  $27.95 \pm 0.16$  Ma. This suggests that the marine and fluvial beds at the Rancho La Palma locality are late Rupelian in age and not lower Miocene as previously reported. Therefore, the marine deposits from the Cerro El Divisadero section can be correlated with the Oligocene El Cien Formation at San Juan de La Costa and are contemporaneous with the middle part of its San Juan Member, representing a marginal facies of this unit. Our results constrain the age of the baleen whales found at the Cerro El Divisadero section, providing clues for Oligocene cetacean evolution in the North Pacific.

**Keywords:** marine-fluvial stratigraphy, U–Pb geochronology, zircon dating.

## RESUMEN

Depósitos marinos costeros y fluviales, expuestos en el Cerro El Divisadero cerca del Rancho La Palma, Baja California Sur, México, contienen registro fósil de cetáceos (ballenas barbadas). La datación de circones de una toba recolectada cerca de la base del Cerro El Divisadero arrojó una edad de  $^{206}\text{Pb}/^{238}\text{U}$  de  $27.95 \pm 0.16$  Ma. Esto sugiere que las capas marinas y fluviales que afloran en la localidad Rancho La Palma son de edad Rupeliano y no del Mioceno temprano como se reportó anteriormente. Por lo tanto, los depósitos marinos del Cerro El Divisadero pertenecen a la Formación El Cien la cual aflora en San Juan de La Costa y son contemporáneos a la parte media del Miembro San Juan, representando una posible facies marginal de esta unidad. Nuestros resultados restringen la edad de los fósiles de ballenas barbadas recolectados en la sección Cerro El Divisadero, proporcionando pistas sobre la evolución de los cetáceos del Oligoceno en el Pacífico Norte.

**Palabras clave:** estratigrafía marina-fluvial, geocronología U–Pb, datación de circones.

### How to cite this article:

Rochín-Bañaga, H., Davis, D.W., Schwennicke, T., Hernández-Cisneros, A.E., 2024, Age constraints on marine-fluvial deposits at Rancho La Palma, Baja California Sur, Mexico: Boletín de la Sociedad Geológica Mexicana, 76 (3), A040424. <http://dx.doi.org/10.18268/BSGM2024v76n3a040424>

Manuscript received: January 30, 2024  
Corrected manuscript received: March 30, 2024  
Manuscript accepted: April 4, 2024

Peer Reviewing under the responsibility of  
Universidad Nacional Autónoma de México.

This is an open access article under the CC BY-NC-SA license  
(<https://creativecommons.org/licenses/by-nc-sa/4.0/>)

## 1. Introduction

Marine sedimentary deposits in the southern Baja California Peninsula show an extensive record of extinct marine vertebrates, including cetacean fossils (Hernández-Cisneros and Nava-Sánchez, 2022; Viglino *et al.*, 2023). A new study at the Rancho La Palma locality, Baja California Sur, Mexico, reports the presence of a new species of a cetacean fossil (*Echericetus novellus*; Hernández-Cisneros *et al.*, 2023) belonging to the Eomysticetidae family, an extinct lineage of baleen whales that lived during the Oligocene.

The Oligocene (33.9–23.0 Ma) is marked by high adaptive radiation in cetacean evolutionary history (*e.g.*, Fordyce, 2017), hence the importance of precise ages to improve our knowledge of timing, duration and processes that drove cetacean evolution.

The discovery of baleen whale fossils at the Rancho La Palma locality attracts interest in understanding the geological context of the marine and fluvial deposits from the Cerro El Divisadero section. The cetacean fossil record within the continuous and well-exposed sedimentary succession from the Cerro El Divisadero makes this a unique locality that brings valuable information for studies of diversification of baleen whales.

However, the lack of absolute ages in many fossiliferous localities makes it challenging to unravel and accurately explain ecological succession events and evolutive changes regarding marine fossil assemblages at southern Baja California peninsula. The beds from Cerro El Divisadero have been informally dated as lower Miocene based on correlation of near volcanic and sedimentary deposits (Schwennicke *et al.*, 1996).

Here we report U-Pb zircon dating of a tuff horizon using laser ablation inductively coupled plasma mass spectrometry (LA-ICPMS). This is the first date to be measured from Cerro El Divisadero section at the Rancho La Palma locality, La Paz, Baja California Sur, Mexico (Figure 1)

### 1.1. STRATIGRAPHIC SETTING

The tuff sample used here for U-Pb dating belongs to a lenticular reworked tuff up to 15 cm thick located above the basal marine deposits (bed 1, 2) of the Cerro El Divisadero stratigraphic section (Figure 1). Schwennicke *et al.* (1996) divided the stratigraphic section at the Cerro El Divisadero into three parts. The basal part represents the marine beds, mudstone and phosphatic sandstone that contains cetacean fossils, the lower part is composed of light-coloured tuffaceous sandstone with conglomeratic lenses, and the upper part consists of grey-brown conglomeratic tuffaceous sandstones. The marine deposits at the Cerro El Divisadero overlie eolian sandstones of the Salto Formation (Schwennicke *et al.*, 1996; Figure 1).

Following Schwennicke *et al.* (1996) and our new observations, the bottom layer (bed 1) is a sandy conglomerate which grades laterally into conglomeratic sandstone representing a gravelly beach deposit and marking the beginning of a marine transgression. This basal conglomeratic bed contains phosphatic grains and grades upwards into sandstone, mudstone, and greenish tuffaceous mudstone with sandstone lenses (bed 2), exhibiting parallel lamination, some lenticular and flaser bedding, and poor bioturbation.

Bed 2 reflects a lagoonal depositional environment influenced by volcanic activity, changing texturally upwards into the grey, slightly tuffaceous volcanioclastic sandstone of bed 3, which is 30 m thick (Schwennicke *et al.*, 1996). Bed 3 reflects a distal fluvial depositional setting. It comprises regularly sorted, silty fine-grained sandstone to poorly sorted, fine to coarse-grained sandstone.

The silty sandstone is predominantly found in the lowermost portion of bed 3 (see Schwennicke *et al.*, 1996). Scattered volcanic granules and pebbles occur in the rock or from thin conglomeratic lenses. The lowermost 2 m of bed 3 typically are finely laminated, and the cross-bedding and cross-lamination are present in the middle and upper parts. Bed 3 grades upwards into coarser muddy, and pebbly sandstone, all of volcanioclas-

Generalized stratigraphy  
of the Cerro El Divisadero section

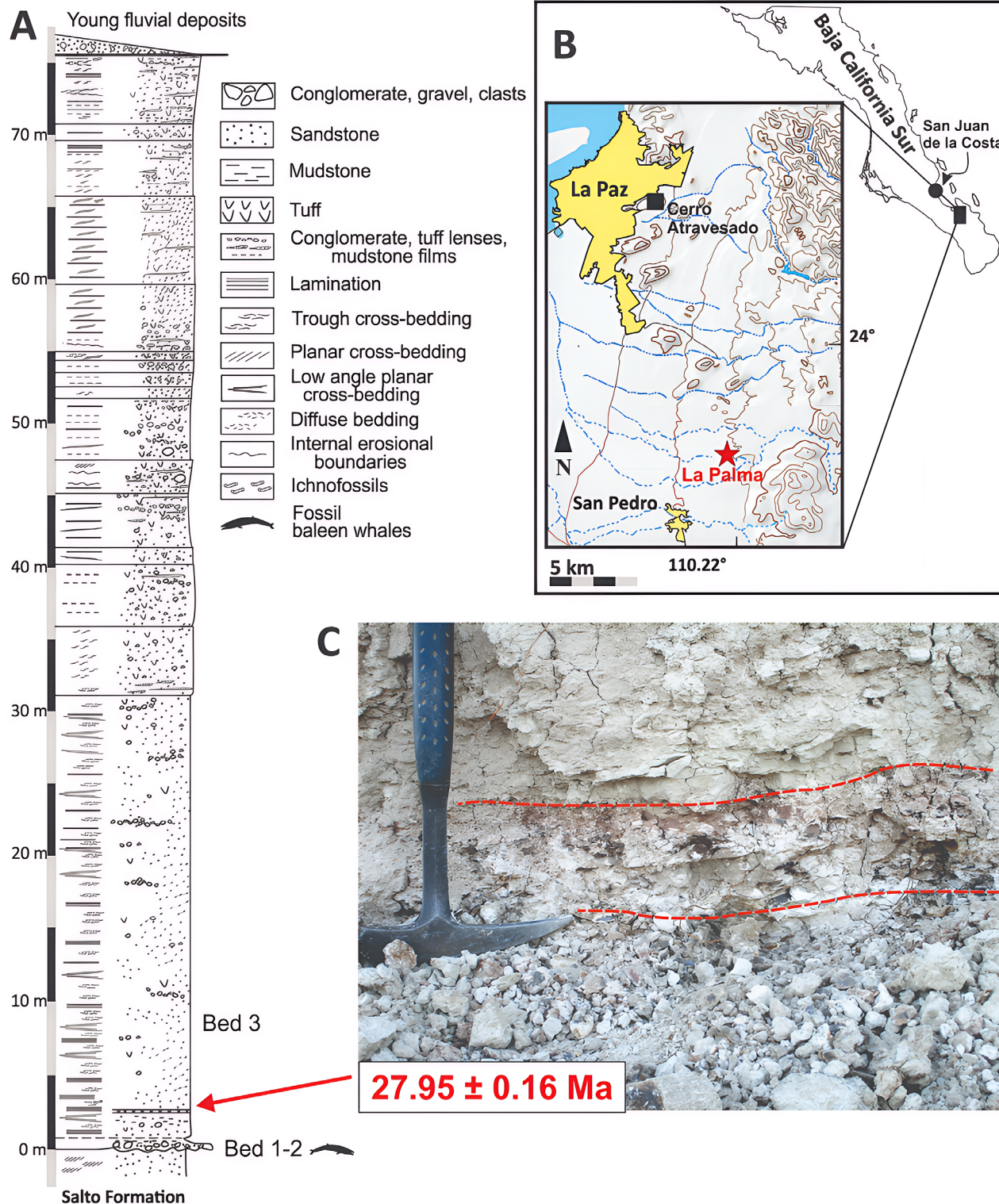


**Figure 1** Study site. A. Stratigraphic column from the Cerro El Divisadero at La Palma locality (after Schwennicke *et al.*, 1996). B. Location of La Palma locality, southern Baja California Peninsula, Mexico (red star). C. Shows the tuff sample used here for U-Pb dating.

tic composition (Figure 1). The fluvial deposits of bed 3 are interpreted herein as basal strata of the volcaniclastic arc-derived Comondú Group, originally defined and described as a formation by Heim (1922) and Hausback (1984).

## 2. Methodology

Zircon grains were separated using standard gravimetric and magnetic separation techniques at the Jack Satterly Laboratory, University of Toronto. Zircon grains and standards were mounted in an epoxy stub and polished to expose the grains. Cathodoluminescence images were used to identify growth zones and inclusions as well as targeting the spot locations (Figure 2).

U–Pb isotopic analyses were conducted using an Agilent 7900 ICPMS and an NWR193 excimer laser system. U–Pb data were collected on  $^{88}\text{Sr}$  (10 ms),  $^{206}\text{Pb}$  (30 ms),  $^{207}\text{Pb}$  (80 ms),  $^{208}\text{Pb}$  (10 ms) and  $^{235}\text{U}$  (20 ms) using spot analyses and were conducted with laser wavelength of 193 nm.  $^{235}\text{U}$  was monitored instead of  $^{238}\text{U}$  in order to remain below the digital to analog detector threshold.

To remove surface contamination, each spot was pre-ablated with ten laser shots using a larger beam size. Laser beam diameter was 50  $\mu\text{m}$ , with a fluence of about 4 J/cm<sup>2</sup> and frequency of 10 Hz. Single spot analysis contained 15 sec background acquisition followed by 25 sec data acquisition and 20 sec washout. Zircon 91500 (Wiedenbeck *et al.*, 1995) standard was used between analyses to correct for plasma mass and oxide elemental fractionation biases.

Temora zircon (Black *et al.*, 2004) was used as a secondary standard with a measured age of  $416.6 \pm 3.4$  Ma ( $2\sigma$ , MSWD = 0.91; Figure S1 in Supplementary Data). Raw data reduction was carried out using custom VBA (Visual Basic for Applications) software written by D.W. Davis. Averaging and regression were carried out using Isoplot (Ludwig, 2012). U decay constants are from Jaffey *et al.* (1971).

## 3. Results and Discussion

The tuffaceous sample yielded fresh-looking zircon grains of euhedral long-prismatic morphology (Figures 2 and 3). Cathodoluminescence images (CLI) show oscillatory zonation, which is typical of felsic igneous rocks (Corfu *et al.*, 2003). Results of 27 analyses on 22 crystals are presented in Supplementary Data (Table S1). A Wetherill concordia plot of U–Pb data is shown in Figure 3. Omitting the oldest analysis, it gives a weighted mean  $^{206}\text{Pb}/^{238}\text{U}$  age of  $27.95 \pm 0.16$  Ma ( $2\sigma$ , MSWD = 1.7). Including the oldest does not change the age significantly ( $27.99 \pm 0.17$  Ma) but it raises the MSWD to 2.1, therefore we have omitted this analysis. The zircon grains show uniform color and morphology (Figure 3). Commonly, detrital zircon grains show variation in color, morphology and size as well as evidence of rounding by transport. Therefore, the uniform age of  $27.95 \pm 0.16$  Ma obtained here from the zircon likely represents an age of volcanic deposition during sedimentation of the marine-fluvial deposits at Rancho La Palma locality (Figure 1).

The Oligocene age of  $27.95 \pm 0.16$  Ma reported here for the Cerro El Divisadero section is significantly older than the inferred Lower Miocene age (younger than 23.0 Ma) suggested by Schwennicke *et al.* (1996). These authors correlated the volcaniclastic rocks from the upper part of the Cerro El Divisadero section with volcanoclastic deposits of the Comondú Formation (Hausback, 1984; Drake *et al.*, 2017; Camarena-Vázquez, 2018) exposed at the Cerro Atravesado near the city of La Paz, about 28 km north of Rancho La Palma (Figure 1), which are overlain by a rhyodacite flow, Comondú Formation, dated with K–Ar at  $19.1 \pm 1.2$  Ma (Hausback, 1984). However, at Cerro Atravesado there are no strata that could be correlated with the marine deposits from the Cerro El Divisadero section at Rancho La Palma locality.

The nearest Oligocene marine deposits to the Cerro El Divisadero section belong to the San Juan Member of El Cien Formation (Fischer *et al.*, 1995) exposed in the area around San Juan de

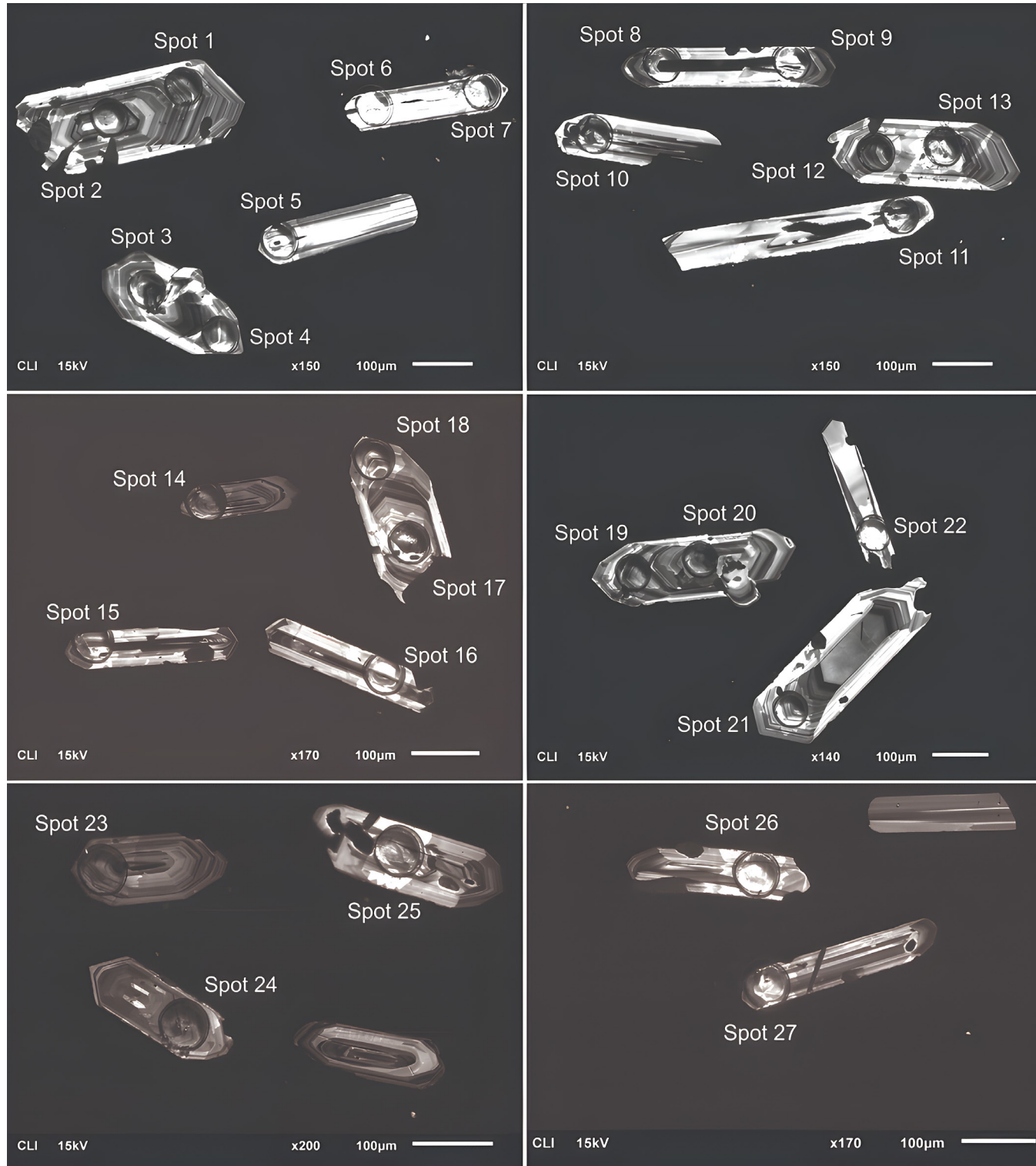
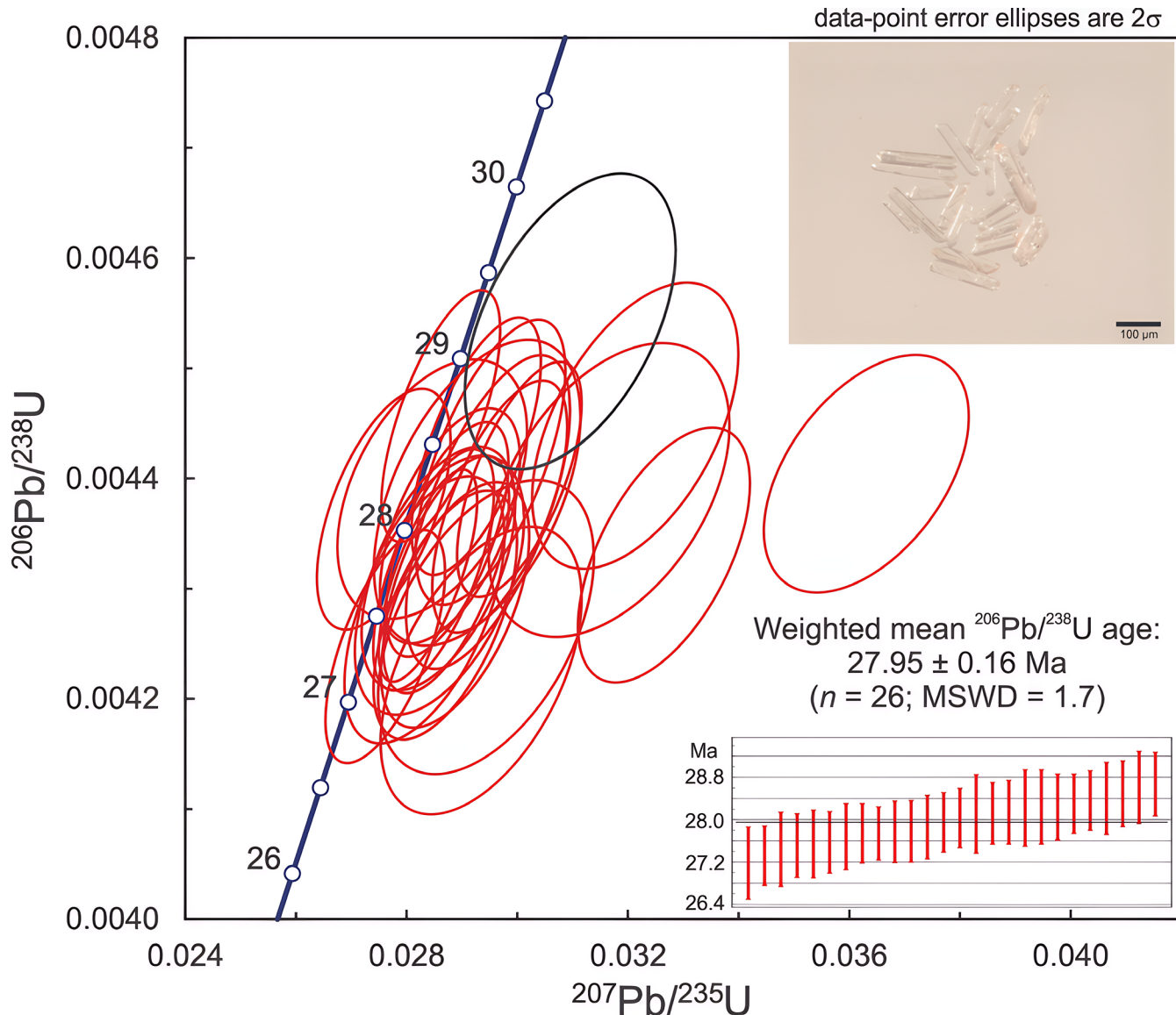


Figure 2 Cathodoluminescence images of ablated representative zircon grains from the tuff sample collected at Cerro El Divisadero.

la Costa, ~40 km northwest of La Paz (Figure 1). The Cien Formation is composed of siliceous and silty mudrock, fine-to coarse-grained sandstone, tuff, coquina beds, conglomerate, and phosphatic sediment (Applegate, 1986; Schwennicke, 1992; Fischer *et al.*, 1995) and is Oligocene in age (Drake *et al.*, 2017; Schöllhorn *et al.*, 2020). Zircon age dating from tuff horizons from the San Juan Member (El Cien Formation) at San Juan de la Costa yield  $^{206}\text{Pb}/^{238}\text{U}$  ages between  $28.6 \pm 0.5$  Ma and  $26.9 \pm$

$0.5$  Ma (Schöllhorn *et al.*, 2020). These Oligocene ages overlap with our results indicating that the marine-fluvial deposits from Cerro El Divisadero section are contemporaneous in age with the San Juan Member at San Juan de La Costa, suggesting that deposition of both sedimentary successions was influenced by the same volcanic activity of the Comondú arc, but deposited under different depositional conditions.

The basal part of the Cerro El Divisadero



**Figure 3** Wetherill concordia diagram showing U-Pb data for single zircon crystals from the tuff bed, Cerro El Divisadero, Rancho La Palma Baja California Sur, Mexico. The black ellipse is omitted from the age regression model.

section shows some palaeontologic and lithologic similarities to the marine beds from El Cien Formation. Marine deposits from the El Cien Formation, the latter includes phosphatic sandstone and phosphorite horizons (*e.g.*, Fischer *et al.*, 1995; Plata-Hernández, 2002; Schöllhorn *et al.*, 2020) as well as abundant vertebrate fossils such as cetaceans (*e.g.*, Hernández-Cisneros *et al.*, 2017). However, despite the cetacean fossil content and the phosphatic material present in the marine beds of the Cerro El Divisadero section, there is no lithological correlation with the marine deposits from the El Cien Formation (San Juan Member). The occurrence of phosphorite horizons (*e.g.*, Fischer *et al.*, 1995; Schöllhorn *et al.*, 2020), diatoms (Kim and Barron, 1986) as well as abundant marine vertebrate fossils, including desmostylians and cetaceans (Grimm, 1992; Hernández-Cisneros *et al.*, 2017), suggest that the marine succession from the middle San Juan Member reflects open shelf-near coast and upwelling area deposits. Conversely, the marine-fluvial beds exposed at Cerro El Divisadero correspond to lagoonal - distal alluvial fan deposits (Schwennicke *et al.*, 1996).

Therefore, the marine deposits at La Palma locality might represent lagoonal and beach settings controlled by a short-lived marine transgression followed by regression due to volcaniclastic influx. These lagoonal-beach facies at La Palma locality are coeval with the middle San Juan Member but are not exposed in the San Juan de La Costa area.

The late Rupelian age of  $27.95 \pm 0.16$  Ma reported here constrains the age of the marine and fluvial deposits from the Cerro El Divisadero as well as the paleontological record of baleen whales. This provides more clues to understand the regional marine palaeoenvironment and facilitates accurate paleontological correlations with other Oligocene localities around the world that contain marine fossil assemblages (*e.g.*, cetacean faunas).

The Oligocene marine deposits in southern Baja California are unique due to their marine mammal fossil content, making them crucial for

the studying the North Pacific biota evolutionary history.

## 4. Conclusions

A U-Pb age of  $27.95 \pm 0.16$  Ma is reported and interpreted here to constrain the time of marine and fluvial deposition from Cerro El Divisadero section at Rancho La Palma locality, Baja California Sur, Mexico. This Oligocene age is in good agreement with U-Pb ages reported from similar tuff horizons in the middle San Juan Member at San Juan de la Costa locality suggesting that the marine deposits from the Cerro El Divisadero section belong to the El Cien Formation.

We conclude that the marine beds in the study area are contemporaneous to the middle part of the San Juan Member and may represent a marginal facies of this unit. The fluvial deposits above are therefore interpreted as basal strata of the volcaniclastic arc-derived Comondú Group. In addition, the age of  $27.95 \pm 0.16$  Ma constrains the paleontological record of cetacean fossils found at the Cerro El Divisadero, helping to understand the evolution of baleen whales in the North Pacific.

## Contributions of authors

(1) Fieldwork: TS; (2) Analysis and data acquisition: HRB, DWD; (3) Methodologic/technical development: HRB, DWD; (4) Writing of the original manuscript and interpretation: HRB, DWD, AEHC, TS.

## Acknowledgements

This study was supported by Natural Sciences and Engineering Research Council of Canada (NSERC), Discovery Grant RGPIN-2016-05575 to D.W. Davis. We are grateful for constructive comments by Luigi Solari and an anonymous reviewer, which greatly improved the manuscript.

## Conflicts of interest

We declare that there is no conflict of interest that could influence the work reported in this paper.

## Handling editor

Francisco J. Vega.

## References

- Applegate, S.P., 1986, The El Cien Formation, strata of Oligocene and early Miocene age in Baja California Sur: *Revista Mexicana de Ciencias Geológicas*, 6(2), 145-162.
- Black, L.P., Kamo, S.L., Allen, C.M., Davis, D.W., Aleinikoff, J.N., Valley, J.W., Mundil, R., Campbell, I.H., Korsch, R.J., Williams, I.S., Foudoulis, C., 2004, Improved  $^{206}\text{Pb}/^{238}\text{U}$  microprobe geochronology by the monitoring of a trace-element-related matrix effect; SHRIMP, ID-TIMS, ELA-ICP-MS and oxygen isotope documentation for a series of zircon standards: *Chemical Geology*, 205(1-2), 115-140. <https://doi.org/10.1016/j.chemgeo.2004.01.003>
- Camarena-Vázquez, J.G., 2018, Análisis de litofacies y posible correlación de las ignimbritas presentes en las regiones del archipiélago Espíritu Santo, San Juan de La Costa y La Paz, B.C.S., México: Baja California Sur, México, Universidad Autónoma de Baja California Sur, tesis de maestría, 199 p.
- Corfu, F., Hanchar, J.M., Hoskin, P.W.O., Kinny, P., 2003, Atlas of zircon textures: *Reviews in Mineralogy and Geochemistry*, 53(1), 469-500. <https://doi.org/10.2113/0530469>
- Drake, W.R., Umhoefer, P.J., Griffiths, A., Vlad, A., Peters, L., McIntosh, W., 2017, Tectono-stratigraphic evolution of the Comondú Group from Bahía de La Paz to Loreto, Baja California Sur, Mexico: *Tectonophysics*, 719-720, 107-115, 123-134. <https://doi.org/10.1016/j.tecto.2017.04.020>
- Fischer, R., Galli-Olivier, C., Gidde, A., Schwennicke, T., 1995, The El Cien Formation of southern Baja California, Mexico: Stratigraphic precisions: *Newsletters on Stratigraphy*, 32(3), 137-161. <https://doi.org/10.1127/nos/32/1995/137>
- Fordyce, R.E., 2017, Cetacean evolution, in Würsig, B., Thewissen, J.G.M., Kovacs, K.M. (eds.), *Encyclopedia of marine mammals*: Cambridge, Mass., Academic Press, 180-185. <https://doi.org/10.1016/B978-0-12-804327-1.00088-1>
- Grimm, K.A., 1992, The sedimentology of coastal upwelling systems: Santa Cruz, California: USA, University of California, PhD dissertation, 862 p.
- Hausback, B.P., 1984, Cenozoic volcanic and tectonic evolution of Baja California Sur, Mexico, in Frizzell Jr., V.A. (ed.), *Geology of the Baja California Peninsula*: USA, Oklahoma, Society of Economic Paleontologists and Mineralogists, Pacific Section, 219-236.
- Heim, A., 1922, Notes on the Tertiary of southern Lower California: *Geological Magazine*, 59(12), 529-547. <https://doi.org/10.1017/S0016756800109069>
- Hernández-Cisneros, A.E., González Barba, G., Fordyce, R.E., 2017, Oligocene cetaceans from Baja California Sur, Mexico: *Boletín de la Sociedad Geológica Mexicana*, 69(1), 149-173. <https://doi.org/10.18268/bsgm2017v69n1a7>
- Hernández-Cisneros, A.E., Nava-Sánchez, E.H., 2022, Oligocene Dawn Baleen Whales in Mexico (Cetacea, Eomysticetidae) and Palaeobiogeographic Notes: *Paleontología Mexicana*, 11(1), 1-12.
- Hernández-Cisneros, A. E., Schwennicke, T., Rochín-Bañaga, H., Cheng-Hsiu, T., 2023, *Echericetus novellus* n. gen. n. sp. (Cetacea: Mysticeti: Eomysticetidae), a late Oligocene baleen whale from Baja California Sur, Mexico: *Journal of Paleontology*, 97(6), 1309-1328. <https://doi.org/10.1017/jpa.2023.80>

- Jaffey, A.H., Flynn, K.F., Glendenin, L.E., Bentley, W.C., Essling, A.M., 1971, Precision measurement of half-lives and specific activities of  $^{235}\text{U}$  and  $^{238}\text{U}$ : Physical Review C, 4(5), 1889-1906. <https://doi.org/10.1103/physrevc.4.1889>
- Kim, W. H., Barron, J. A., 1986, Diatom biostratigraphy of the upper Oligocene to lowermost Miocene San Gregorio Formation, Baja California Sur, Mexico: Diatom Research, 1(2), 169–189. <https://doi.org/10.1080/0269249X.1986.9704967>
- Ludwig, K.R., 2012, User's manual for Isoplot 3.75: A geochronological toolkit for Microsoft Excel: Berkeley Geochronological Center Special Publication, 4, 75 p.
- Plata-Hernández, E., 2002, Cartografía y estratigrafía del área de Tembabichi: Baja California Sur, México: Baja California Sur, México, Universidad Autónoma de Baja California Sur, Área Interdisciplinaria de Ciencias del Mar, Departamento de Geología Marina, tesis de licenciatura, 113 p.
- Schöllhorn, I., Houben, A., Gertsch, B., Adatte, T., Alexey, U., de Kaenel, E., Spangenberg, J.E., Janssen, N., Schwennicke, T., Föllmi, K.B., 2020, Enhanced upwelling and phosphorite formation in the northeastern Pacific during the late Oligocene: Depositional mechanisms, environmental conditions, and the impact of glacio-eustacy: Geological Society of America Bulletin, 132(3-4), 687-709. <https://doi.org/10.1130/B32061.1>
- Schwennicke, T., 1992, Phosphoritführende Tief- und Flachwassersedimente aus dem Oberoligozän von Niederkalifornien, Mexiko: Die San Juan-Einheit (El Cien Formation): Hannover, Germany, Universität Hannover, doctoral thesis, 163 p.
- Schwennicke, T., González-Barba, G., and de Anda-Franco, N. 1996, Lower Miocene marine and fluvial beds at rancho La Palma, Baja California Sur, México: Boletín del Departamento de Geología de la Universidad de Sonora 13(1): 1–14.
- Viglino, M., Valenzuela-Toro, A.M., Benites-Palomino, A., Hernández-Cisneros, A.E., Gutstein, C.S., Aguirre-Fernández, G., Vélez-Juarbe, J., Cozzuol, M.A., Buono, M.R., Loch, C., 2023, Aquatic mammal fossils in Latin America – a review of records, advances and challenges in research in the last 30 years: Latin American: Journal of Aquatic Mammals, 18(1), 50-65. <https://doi.org/10.5597/lajam00295>
- Wiedenbeck, M., Alle, P., Corfu, F., Griffin, W. I., Meier, M., Oberli, F., Quadri, A. V., Roddick, J. C., Spiegel, W., 1995, Three Natural Zircon Standards for U-Th-Pb, Lu-Hf, Trace Element and Ree Analyses: Geostandards Newsletter, 19(1), 1-23. <https://doi.org/10.1111/j.1751-908X.1995.tb00147.x>

## Supplementary Data

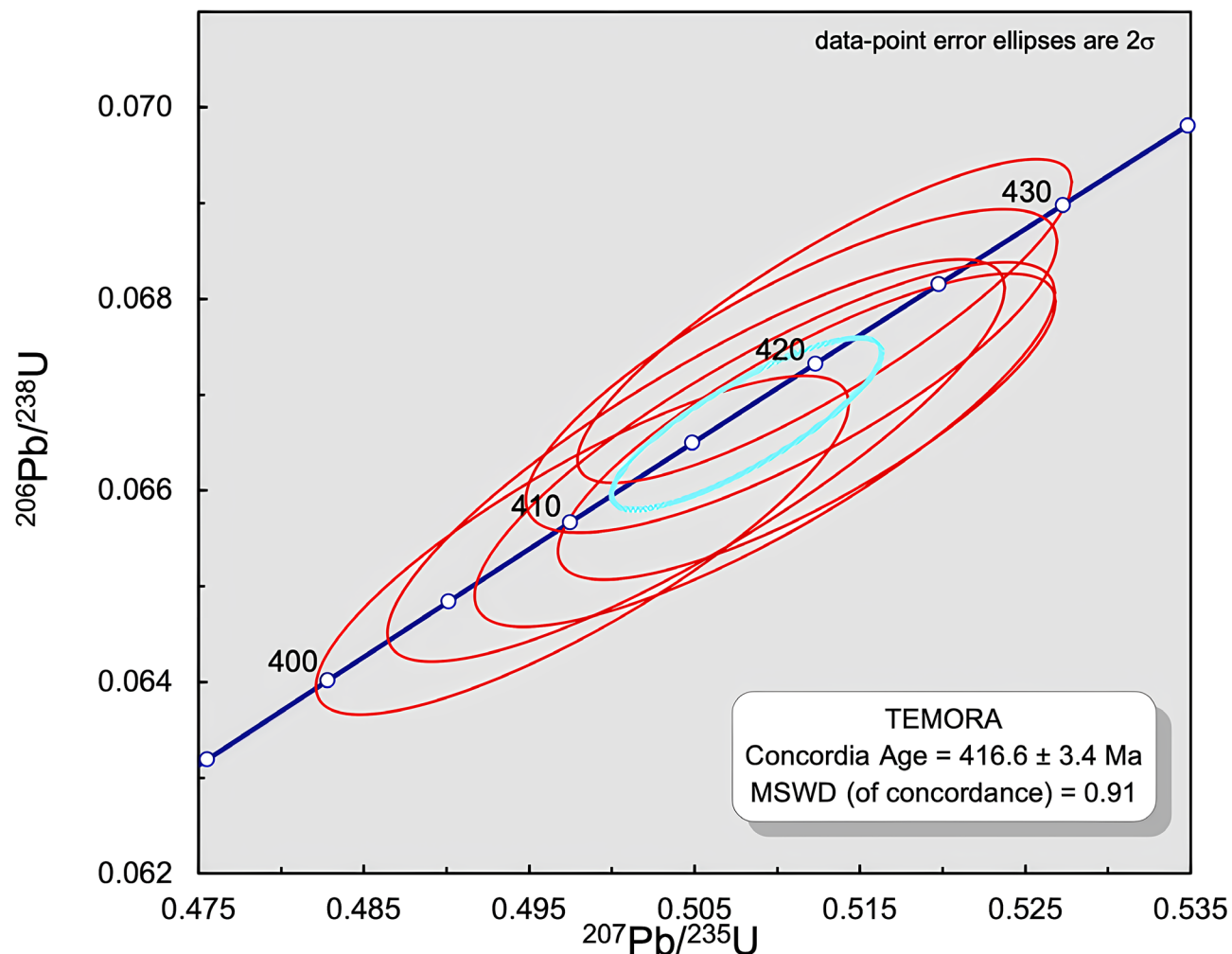


Figure S1 | Wetherill concordia diagram showing U-Pb data for Temora zircon.

**Table S1.** U-Pb zircon data from Cerro El Divisadero near Rancho La Palma locality southern Baja California Peninsula, Mexico.

Standardized Concordia:										Ages Ma							
Analysis	207Pb/235U	SigM	206Pb/238U	SigM	RhoXY	U ppm	206Pb ppm	Th/U	207Pb/206Pb	SigM	207Pb/235U	SigM	206Pb/238U	SigM	%Disc		
Spot 1	0.02832138	0.0006	0.0043	0.00005	0.554	386	1.65	0.5	98.44	40.66	28.36	0.58	27.54	0.32	72		
Spot 2	0.02859344	0.0006	0.0043	0.00005	0.510	337	1.45	0.45	108.76	43.87	28.63	0.62	27.68	0.31	75		
Spot 3	0.02857366	0.0006	0.0043	0.00005	0.527	486	2.1	0.62	98.89	39.42	28.61	0.56	27.78	0.29	72		
Spot 4	0.0316597	0.0009	0.0044	0.00005	0.442	173	0.76	0.8	298.95	56.5	31.65	0.87	28.24	0.35	91		
Spot 5	0.03265113	0.0006	0.0043	0.00005	0.562	415	1.8	0.51	399.26	35.66	32.62	0.62	27.86	0.3	93		
Spot 6	0.02934651	0.0007	0.0042	0.00005	0.499	247	1.05	0.29	212.03	50	29.37	0.73	27.18	0.34	87		
Spot 7	0.02848765	0.0004	0.0043	0.00004	0.661	868	3.75	0.38	92.32	27.64	28.52	0.44	27.77	0.29	70		
Spot 8	0.02871494	0.0005	0.0043	0.00004	0.631	580	2.5	0.34	113.37	29.38	28.75	0.46	27.74	0.28	76		
Spot 9	0.02927348	0.0008	0.0044	0.00006	0.495	236	1.04	0.38	118.59	52.59	29.30	0.75	28.22	0.36	76		
Spot 10	0.02968228	0.0005	0.0044	0.00005	0.636	721	3.15	0.43	157.92	30.06	29.70	0.49	28.14	0.3	82		
Spot 11	0.02878451	0.0005	0.0044	0.00004	0.557	468	2.04	0.37	95.08	34.99	28.81	0.51	28.03	0.28	71		
Spot 12	0.02846352	0.0007	0.0044	0.00005	0.445	323	1.42	0.46	50.33	51.87	28.50	0.69	28.24	0.31	44		
Spot 13	0.03650096	0.0008	0.0044	0.00004	0.482	597	2.63	0.63	604.9	38.85	36.40	0.74	28.36	0.28	96		
Spot 14	0.03213087	0.0008	0.0044	0.00005	0.503	369	1.64	0.64	302.61	46.06	32.11	0.75	28.61	0.34	91		
Spot 15	0.02758434	0.0005	0.0044	0.00004	0.570	688	3.01	0.9	6.482	18.35	27.63	0.49	28.12	0.29	100		
Spot 16	0.02861796	0.0004	0.0045	0.00005	0.683	894	3.99	0.53	27.37	26.72	28.65	0.43	28.67	0.3	-5		
Spot 17	0.03003579	0.0005	0.0044	0.00004	0.647	826	3.63	0.47	172.48	27.05	30.05	0.45	28.3	0.28	84		
Spot 18	0.0309769	0.0008	0.0045	0.00005	0.481	261	1.19	0.71	168.65	50.38	30.98	0.76	29.23	0.35	83		
Spot 19	0.02873362	0.0005	0.0043	0.00004	0.638	740	3.22	0.56	97.54	28.38	28.76	0.45	27.95	0.28	72		
Spot 20	0.02925503	0.0005	0.0044	0.00005	0.660	740	3.28	0.44	94.5	28.83	29.28	0.47	28.49	0.31	70		
Spot 21	0.02951744	0.0006	0.0044	0.00005	0.639	646	2.85	0.48	123.35	33.58	29.54	0.54	28.4	0.34	77		
Spot 22	0.02946952	0.0006	0.0044	0.00006	0.647	483	2.11	0.62	143.78	36.44	29.49	0.6	28.11	0.37	81		
Spot 23	0.02943381	0.0008	0.0043	0.00005	0.471	226	0.97	0.43	197.38	54.63	29.46	0.79	27.44	0.35	86		
Spot 24	0.02838264	0.0004	0.0043	0.00004	0.712	1066	4.6	0.76	86.49	21.26	28.42	0.36	27.74	0.25	68		
Spot 25	0.0276123	0.0004	0.0042	0.00004	0.636	687	2.92	0.48	56.77	29.24	27.66	0.44	27.32	0.28	52		
Spot 26	0.02869834	0.0005	0.0043	0.00005	0.585	643	2.75	0.55	132.27	34.9	28.73	0.52	27.51	0.3	79		
Spot 27	0.02887489	0.0005	0.0043	0.00005	0.559	481	2.06	0.5	141.62	36.56	28.90	0.54	27.57	0.29	81		
<b>Temora zircon</b>																	
Temora-1	0.50507468	0.0076	0.0663	0.00086	0.857	243	16.13	0.64	421.97	17.35	415.13	5.15	413.9	5.2	2		
Temora-2	0.50923848	0.0072	0.0665	0.00078	0.831	208	13.85	0.65	434.59	17.4	417.94	4.82	414.9	4.7	5		
Temora-3	0.51286227	0.0061	0.0678	0.00069	0.857	440	29.83	0.78	407.64	13.71	420.37	4.1	422.7	4.2	-4		
Temora-4	0.51178449	0.0061	0.0667	0.00065	0.815	459	30.58	0.8	439.52	15.47	419.65	4.13	416.0	3.9	6		
Temora-5	0.51084369	0.0066	0.0672	0.00069	0.798	331	22.26	0.66	416.08	17.24	419.02	4.41	419.6	4.2	-1		
Temora-6	0.49821103	0.0066	0.0654	0.00072	0.835	251	16.43	0.67	421.43	16.23	410.49	4.47	408.6	4.4	3		